Adaptive Control for Mechanical Ventilation for Improved Pressure Support

Adaptive Control for Mechanical Ventilation for Improved Pressure Support

Joey Reinders, Bram Hunnekens, Frank Heck, Tom Oomen, *Senior Member, IEEE*, and Nathan van de Wouw, *Senior Member, IEEE*

***Abstract*— Respiratory modules are medical devices used to assist patients to breathe. The aim of this article is to develop a control method that achieves exact tracking of a time-varying target pressure, for unknown patient-hose-leak parameters and in the presence of patient breathing effort. This is achieved by an online estimation of the hose characteristics that enables compensation for the pressure drop over the hose. Stability of the closed-loop system is proven, and the performance improvement compared to the existing control strategies is demonstrated by simulation and experimental case studies.**

***Index Terms*— Adaptive control, mechanical ventilation, medical applications, respiratory systems, tracking performance.**

I. Introduction

MECHANICAL ventilation is commonly used in intensive care units (ICUs) to assist patients who need support to breathe sufficiently. The main goals of mechanical ventilation are to ensure oxygenation and carbon dioxide elimination [1]. A large number of patients require mechanical ventilation. According to [2], 19 186 people required mechanical ventilation in ON, Canada, in 2000. Therefore, improvements of ventilation benefit a large population worldwide.

The goal of mechanical ventilation is achieved using a mechatronic system, the mechanical ventilator. A schematic overview of a mechanical ventilator, with a single-hose setup and a patient, is shown in Fig. 1. In this article, blower-driven pressure-controlled ventilation (PCV) of sedated patients and continuous positive airway pressure (CPAP) ventilation of spontaneously breathing patients is considered.

Manuscript received May 20, 2019; revised December 3, 2019; accepted January 15, 2020. Date of publication February 18, 2020; date of current version December 17, 2020. Manuscript received in final form January 22, 2020. Recommended by Associate Editor Y. Pan. *(Corresponding author: Joey Reinders.)*

Joey Reinders is with Demcon Advanced Mechatronics, Best, The Netherlands, and also with the Department of Mechanical Engineering, Eindhoven University of Technology, Eindhoven, The Netherlands (e-mail: joey.reinders@demcon.nl).

Bram Hunnekens is with Demcon Advanced Mechatronics, Best, The Netherlands (e-mail: bram.hunnekens@demcon.nl).

Frank Heck is with Demcon Macawi Respiratory Systems, Best, The Netherlands (e-mail: frank.heck@demcon.nl).

Tom Oomen is with the Department of Mechanical Engineering, Eindhoven University of Technology, Eindhoven, The Netherlands (e-mail: t.a.e.oomen@tue.nl).

Nathan van de Wouw is with the Department of Mechanical Engineering, Eindhoven University of Technology, Eindhoven, The Netherlands, and also with the Department of Civil, Environmental and Geo-Engineering, University of Minnesota, Minneapolis, MN 55455 USA (e-mail: n.v.d.wouw@tue.nl).

Color versions of one or more of the figures in this article are available online at https://ieeexplore.ieee.org.

Digital Object Identifier 10.1109/TCST.2020.2969381

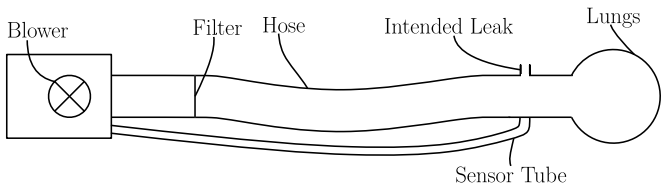

Fig. 1. Schematic of the blower-hose-patient system of the considered positive pressure ventilation system.

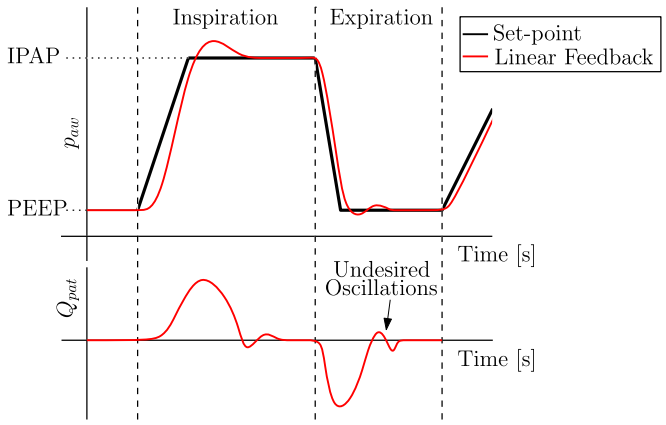

Fig. 2. Airway pressure and patient flow during one breathing cycle of PCV (p_{aw}: airway pressure and Q_{pat}: flow into the patient's lungs, see also Fig. 5).

In PCV, the blower compresses ambient air to achieve the desired pressure profile (Fig. 2) near the patient's mouth. The blower is increasing the airway pressure during inspiration, to achieve the inspiratory positive airway pressure (IPAP), filling the patient's lungs with air. After a preset amount of time has passed, the blower decreases the pressure to the positive end-expiratory pressure (PEEP) such that the lungs are emptied.

In CPAP, the goal is to achieve a continuous airway pressure, while the patient breaths through this profile. A substantial amount of research has been conducted to obtain the optimal ventilator settings and modes [3]–[5], which focuses on the design of the pressure set point.

Accurate tracking of the target pressure is important to achieve sufficient support for the patient, especially in cases of large flows, as a result of large lungs and/or unintentional leaks, e.g., in noninvasive ventilation. Furthermore, accurate pressure tracking results in better patient-ventilator synchrony;

in [6] and [7], it is argued that better tracking prevents false triggers, improving patient-ventilator synchrony. Asynchrony between patient and machine is even associated with high mortality [8]. Finally, for more complex ventilation modes, allowing for patient effort, exact tracking is essential to deliver the required level of assistance more accurately.

Traditionally, these ventilators are controlled using linear time-invariant feedback controllers. This results in suboptimal tracking performance in terms of overshoot and settling time, as shown in Fig. 2. The main cause for such suboptimal performance is the large variety of plants for which the linear feedback controller should be robust. Indeed, the controller should ensure robust performance for a broad spectrum of patients, from infants to adults, varying disposable hose-filter systems, unknown leakage, and possibly unknown patient activity.

Different control strategies have been investigated to improve the mechanical ventilators. In [9], an overview of modeling and control techniques for mechanical ventilation is presented. Variable-gain control is proposed in [6] and [7], which aims to achieve pressure tracking while reducing the overshoot in patient flow, preventing false triggering. This article shows a clear reduction in patient flow overshoot. However, still, some overshoot is present and the patient flow is used in the control strategy, which is typically not available. In [10], an adaptive feedback control approach is applied, which is estimating the patient model and using this to adaptively tune a controller that achieves a desired closed-loop transfer function. In theory this works well, however, in practice it is complex to obtain an accurate patient model. Furthermore, in [10], the hose resistance is neglected, while for large air flows, induced by large lungs and/or leakage, the hose-induced pressure drop cannot be neglected. Also, funnel-based control [11] is applied to mechanical ventilation; however, the obtained gain in tracking performance is limited. In [12], a model-based control approach is used, and in [13], a model predictive control approach is applied. These methods require accurate patient parameters that are typically not available in practice. Furthermore, iterative learning control [14] is applied to mechanical ventilation. This article shows a significant improvement in tracking performance. A drawback of this approach is that it is limited to repeated sequences of the set point and initial conditions. Therefore, the performance of the iterative learning control framework proposed in [14] degrades when patients are breathing spontaneously.

Although previous research shows promising improvements in tracking performance, it does not achieve sufficiently accurate tracking of the target pressure, for the required range of patients, patient effort, hose-filter systems, and set points. To achieve this, this article presents an adaptive control strategy that compensates for the pressure drop over the hose. A hose resistance estimate and the measured output flow are used to compensate for the pressure drop over the hose. Manual calibration of the hose-filter system to obtain the hose resistance is an undesired option because of the already increasing demand of health care and the lack of trained personnel (see [2], [15]). Furthermore, the hose resistance might change during ventilation, due to clogging of the filter. Therefore, an online recursive least squares (RLS) estimator is developed to estimate the hose resistance automatically during ventilation.

In this article, an adaptive control scheme is considered instead of a robust scheme. First, the wide variety of patients and hose types leads to a situation where it is challenging to achieve adequate performance for every patient using one single robustly tuned linear feedback controller. Second, manual calibrations are undesired because of the lack of time in a hospital setting; such calibration can be omitted by using an adaptive controller. Third, since the system parameters may vary over time, it is beneficial that an adaptive scheme responds to such variations, thereby guaranteeing high performance under such changing circumstances.

The main difference with the adaptive control strategy in [10] is that, in the proposed control strategy, only the hose-resistance model is estimated and used in the feedback loop. The patient parameters are not estimated, which is typically challenging because of the wide variety of patients and the model uncertainty concerning the structure of the patient model. Therewith, the method proposed in this article is invariant to the patient model, which is a significant advantage over the adaptive control scheme in [10].

The main contribution of this article is the design of a control strategy for mechanical ventilation, which ensures the exact tracking of the airway pressure independent of the patient, hose, leakage, patient effort, and set point. Key advantages of the proposed approach include that it allows for a fast and accurate pressure response, even for large lungs and big leaks, prevents overshoot in the patient flow and therewith prevents false triggering, and is not using direct feedback on the patient airway pressure, improving robustness, since the patient airway sensor tube might detach.

The first subcontribution is a stability proof of the resulting closed-loop system, ensuring exponential convergence of the estimation and tracking errors to zero. As a second subcontribution, a significant improvement in tracking performance in comparison to state-of-practice control strategies is shown through a simulation case study. The third subcontribution is an experimental case study that shows the practical applicability of the controller and improvement over the state-of-practice control strategies.

The outline of this article is as follows. In Section II, the control problem and high-level control approach are described. In Section III, a mathematical model of the patient-hose system is presented. In Section IV, the developed control strategy is described and a stability analysis is presented. A model-based simulation study is presented in Section V, comparing state-of-practice control strategies to the developed adaptive controller. In Section VI, the adaptive controller is compared to state-of-practice control strategies in an experimental case study. Finally, the conclusions and recommendations are presented in Section VII.

II. Control Problem Formulation

In this section, the considered system is first presented. Thereafter, the control problem is formulated and the state-of-practice control approach is discussed in this context.

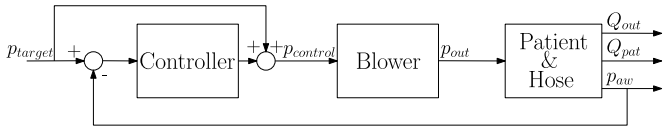

Fig. 3. State-of-practice control scheme of closed-loop linear feedback control with unit feedforward.

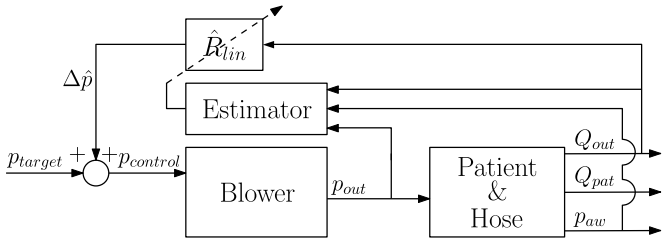

Fig. 4. Schematic of the proposed closed-loop system with an RLS estimator for the hose resistance estimation.

Furthermore, a high-level description of the proposed control approach is given.

A schematic overview of the system, with the most important system components, is shown in Fig. 1. The system is operated by the blower, which pressurizes ambient air in order to ventilate the patient. A hose is used to connect the respiratory module to the patient. The flow, which leaves the blower, runs through the hose toward the patient. The patient exhales partly back through the blower and partly through a leak in the hose near the patient's mouth (see Fig. 1). This leak is used to refresh the air in the hose, ensuring that the patient does not inhale previously exhaled, low-oxygen, air.

A. Control Problem and State-of-Practice Approach

In blower-driven respiratory systems, typically, linear integral feedback controllers are used. Implementing a linear feedback controller results in a closed-loop system, as shown in Fig. 3. In this closed-loop system, the airway pressure p_{aw} is the variable to be controlled, i.e., it should track the target pressure p_{target}. The overall control goal is to minimize the tracking error, which is defined as

$$e := p_{\text{target}} - p_{\text{aw}} \tag{1}$$

or ideally let it converge to zero asymptotically.

To achieve a blower output pressure $p_{\text{out}} = p_{\text{control}}$, an accurate lookup table is used in addition to a feedback controller using feedback of the blower error ($p_{\text{control}} - p_{\text{out}}$). This lookup table is used to determine the desired blower RPM to achieve the desired outlet pressure p_{out}, given the measured outlet flow Q_{out}. The feedback controller is used to eliminate the remaining blower error. Combined, the lookup table and the feedback controller accurately achieve $p_{\text{out}} = p_{\text{control}}$ in the frequency domain of interest. Consequently, the unit feedforward in combination with the blower characteristic ensures that p_{out} is exactly tracking p_{target}.

Since unit feedforward achieves $p_{\text{out}} = p_{\text{target}}$, the feedback controller in Fig. 3 has to compensate for the pressure drop $\Delta p = p_{\text{out}} - p_{\text{aw}}$ along the hose. Note that it is challenging to predict the pressure drop along the hose due to several factors.

1) The type of lung attached, i.e., the patient, is in principle unknown. Although the pressure target is *a priori* known, the amount of flow entering a lung depends on the lung resistance and lung compliance and is therefore unknown. Therewith, also the flow through the hose and, thus, the pressure drop Δp are unknown.
2) The characteristic of the hose system attached is also unknown. Hence, the pressure drop along the hose is unknown.
3) During (noninvasive) ventilation, there can be leakage around the mask, which cannot be predicted and therefore results in an *a priori* unknown pressure drop.
4) In addition, patients can have spontaneous breathing activity (resulting in a flow and therewith a pressure drop along the hose), which also cannot be predicted *a priori*.

Therefore, exact feedforward control cannot be used to compensate for the pressure drop Δp over the hose.

Alternatively, a linear feedback controller, typically a proportional–integral (PI) controller, is used to compensate for the pressure drop over the hose. A linear feedback controller has to be tuned for robustness over large plant variations. Therefore, it is unable to achieve accurate tracking for all considered patients. Furthermore, a feedback controller uses the measured airway pressure p_{aw} in the feedback loop. Feedback on p_{aw} is undesired since the sensor tube might get detached in practice.

B. Proposed Control Strategy

Here, a control strategy is proposed that uses an estimated hose resistance model and the output flow Q_{out}, which is measured near the blower, to compensate for the pressure drop Δp over the hose (see Fig. 4). Because the hose resistance is unknown, an offline calibration could be conducted by hospital personnel to estimate the hose resistance prior to ventilation. This calibration requires extra time of the hospital staff, which is undesired because of the already existing lack of time for hospital staff, as mentioned in Section I. Furthermore, the resistance may change over time.

Therefore, an adaptive control approach is developed, which is using an online RLS estimator to estimate the hose resistance automatically during ventilation (see Fig. 4). Practically, this approach is considerably more reliable than the state-of-practice feedback method, which is using p_{aw} directly in the feedback loop. The proposed strategy is only using p_{aw} for updating the estimator. In practice, the sensor tube used to measure p_{aw} might get detached. In such a scenario, the proposed controller can keep running without updating the resistance, whereas the feedback controller fails and may cause a potentially dangerous situation.

Another advantage of this control strategy is that it compensates for the pressure drop Δp over the hose using the measured blower outlet flow Q_{out}. The pressure drop over the hose Δp depends on the flow through the hose, which is equal to the blower outlet flow Q_{out}. Therefore, exact compensation

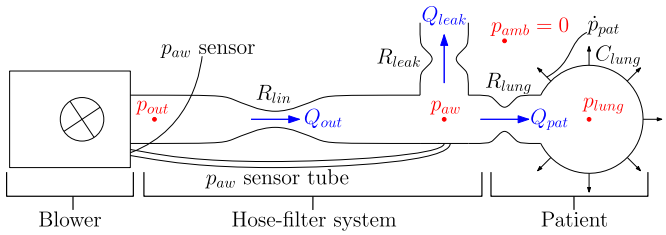

Fig. 5. Schematic of the blower-hose-patient system, with the corresponding resistances, lung compliance, and patient effort.

of this pressure drop based on the measured flow allows for perfect tracking independent of the leak, patient dynamics, and patient effort. In Section III, a model of the patient-hose dynamics is presented.

III. Patient-Hose Dynamics

In this section, a description of the system parameters used in the model is given. Thereafter, the open-loop patient-hose dynamics are presented.

A. Patient-Hose Parameters

Before presenting the mathematical model, the system parameters and their physical meaning are discussed. Consider the schematic of the blower, hose, and patient shown in Fig. 5. First, the blower compresses ambient air to the desired blower outlet pressure p_{out}. Note that all pressures are defined relative to the ambient pressure, i.e., $p_{\text{amb}} = 0$. This outlet pressure results in a flow Q_{out} through the hose, with resistance R_{lin}. Furthermore, the patient airway pressure p_{aw} is measured just in front of the patient's mouth, using the sensor tube. A leak is used to flush exhaled CO_2-rich air from the hose system and is modeled using the leak resistance R_{leak}. The lung is modeled using a linear one-compartmental lung model as described in [16], with lung compliance C_{lung} and resistance R_{lung}. Note that all physical patient-hose parameters, i.e., R_{lin}, R_{leak}, R_{lung}, and C_{lung}, are strictly positive. Furthermore, Fig. 5 shows the patient's breathing effort $\dot{p}_{\text{pat}}$, which is considered an exogenous disturbance on the lung pressure, caused by the patient's respiratory effort.

B. Patient-Hose Model

Using the parameters and models outlined earlier, a mathematical patient-hose model is derived. This model describes the relation between the blower outlet pressure p_{out}, the disturbance $\dot{p}_{\text{pat}}$, the state p_{lung}, and the outputs p_{aw} and Q_{out}.

Using conservation of flow, the output flow Q_{out}, patient flow Q_{pat}, and leakage flow Q_{leak} are related by

$$Q_{\text{pat}} = Q_{\text{out}} - Q_{\text{leak}}. \tag{2}$$

The resistances are modeled using a linear resistance model, which is reasonably accurate for typical flows in ventilation. Using the linear resistances R_{lin}, R_{leak}, and R_{lung}, the pressures and flows are related as follows:

$$\begin{aligned} Q_{\text{out}} &= \frac{p_{\text{out}} - p_{\text{aw}}}{R_{\text{lin}}} \\ Q_{\text{leak}} &= \frac{p_{\text{aw}}}{R_{\text{leak}}} \\ Q_{\text{pat}} &= \frac{p_{\text{aw}} - p_{\text{lung}}}{R_{\text{lung}}}. \end{aligned} \tag{3}$$

The lung dynamics are governed by

$$p_{\text{lung}}(t) = \frac{1}{C_{\text{lung}}} \int_0^t Q_{\text{pat}} dt + p_{\text{pat}}(t) + p_{\text{lung}}(0) \tag{4}$$

with $p_{\text{pat}}(t)$ the (time-varying) patient effort. The patient effort is modeled as an unknown disturbance on the lung pressure, induced by the patient's respiratory efforts, e.g., diaphragm and/or abdominal muscle contractions. Furthermore, $p_{\text{lung}}(0)$ represents the initial lung pressure, excluding the patient effort. The time derivative of the lung pressure then satisfies

$$\dot{p}_{\text{lung}}(t) = \frac{1}{C_{\text{lung}}} Q_{\text{pat}} + \dot{p}_{\text{pat}}. \tag{5}$$

Combining (3) and (5), the lung dynamics are described by

$$\dot{p}_{\text{lung}} = \frac{p_{\text{aw}} - p_{\text{lung}}}{C_{\text{lung}} R_{\text{lung}}} + \dot{p}_{\text{pat}}. \tag{6}$$

The following relation for the airway pressure is obtained from (2) and (3):

$$p_{\text{aw}} = \frac{R_{\text{lin}} R_{\text{leak}} p_{\text{lung}} + R_{\text{leak}} R_{\text{lung}} p_{\text{out}}}{\bar{R}} \tag{7}$$

with $\bar{R} := R_{\text{lin}} R_{\text{leak}} + R_{\text{lin}} R_{\text{lung}} + R_{\text{leak}} R_{\text{lung}}$. By substituting (7) into (6), a differential equation for the lung dynamics is obtained

$$\dot{p}_{\text{lung}} = \frac{-(R_{\text{lin}} + R_{\text{leak}})}{C_{\text{lung}} \bar{R}} p_{\text{lung}} + \frac{R_{\text{leak}}}{C_{\text{lung}} \bar{R}} p_{\text{out}} + \dot{p}_{\text{pat}}. \tag{8}$$

Given (3), (7), and (8), the patient-hose system dynamics can be written as a linear state-space system with input p_{out}, outputs p_{aw} and Q_{pat}, state p_{lung}, and disturbance $\dot{p}_{\text{pat}}$

$$\begin{aligned} \dot{p}_{\text{lung}} &= \mathbf{A}_h p_{\text{lung}} + \mathbf{B}_h p_{\text{out}} + \dot{p}_{\text{pat}} \\ \begin{bmatrix} p_{\text{aw}} \\ Q_{\text{pat}} \end{bmatrix} &= \mathbf{C}_h p_{\text{lung}} + \mathbf{D}_h p_{\text{out}} \end{aligned} \tag{9}$$

with

$$\begin{aligned} \mathbf{A}_h &= -\frac{R_{\text{lin}} + R_{\text{leak}}}{C_{\text{lung}} \bar{R}}, \quad \mathbf{B}_h = \frac{R_{\text{leak}}}{C_{\text{lung}} \bar{R}} \\ \mathbf{C}_h &= \begin{bmatrix} \frac{R_{\text{lin}} R_{\text{leak}}}{\bar{R}} & -\frac{R_{\text{lin}} + R_{\text{leak}}}{\bar{R}} \end{bmatrix}^T \\ \mathbf{D}_h &= \begin{bmatrix} \frac{R_{\text{leak}} R_{\text{lung}}}{\bar{R}} & \frac{R_{\text{leak}}}{\bar{R}} \end{bmatrix}^T. \end{aligned} \tag{10}$$

Since all resistances and the compliance are strictly positive constants, $\mathbf{A}_h$ is negative and, hence, the patient-hose system is inherently asymptotically stable. Note that $\dot{p}_{\text{pat}}$ is considered to be an exogenous disturbance, whereas, in practice, it contains dynamics, i.e., the patient's breathing behavior.

IV. Adaptive Controller Design and Stability Analysis

In this section, the proposed adaptive control approach is presented, leading to the main contribution of this article. In Section IV-A, the closed-loop dynamics resulting from the new control strategy are presented, for the case in which a constant estimate $\hat{R}_{\text{lin}}$ of the hose resistance R_{lin} is used. In Section IV-B, the RLS estimator, used to estimate the hose resistance, is given. Finally, in Section IV-C, a stability analysis of the resulting closed-loop dynamics, including the estimator, is presented.

A. Closed-Loop Dynamics for a Constant Hose-Resistance Estimate

In this section, a state-space description of the closed-loop dynamics with a constant estimate $\hat{R}_{\text{lin}}$ is derived. This state-space description is needed to analyze the performance and stability of the controlled system. In the closed-loop dynamics, a feedback controller on the blower outlet flow Q_{out} is included, as shown in Fig. 4. The constant feedback controller in Fig. 4 and the fact that the blower gain is 1 in the frequency domain of interest results in $p_{\text{out}} = p_{\text{control}} = \Delta\hat{p} + p_{\text{target}}$. Using $p_{\text{out}} = \Delta\hat{p} + p_{\text{target}}$ and (9) results in

$$\dot{p}_{\text{lung}} = \mathbf{A}_h p_{\text{lung}} + \mathbf{B}_h(p_{\text{target}} + \Delta\hat{p}) + \dot{p}_{\text{pat}}. \tag{11}$$

From Fig. 4, we know that the estimated pressure drop is given by $\Delta\hat{p} = \hat{R}_{\text{lin}} Q_{\text{out}}$. Using (2), (3), and (5), this pressure drop estimate can be rewritten as

$$\begin{aligned}\Delta\hat{p} &= \hat{R}_{\text{lin}} Q_{\text{out}} \\ &= \hat{R}_{\text{lin}}(Q_{\text{pat}} + Q_{\text{leak}}) \\ &= \hat{R}_{\text{lin}}\left(C_{\text{lung}}(\dot{p}_{\text{lung}} - \dot{p}_{\text{pat}}) + \frac{p_{\text{aw}}}{R_{\text{leak}}}\right).\end{aligned} \tag{12}$$

Note that $p_{\text{control}} = \Delta\hat{p} + p_{\text{target}}$ together with (12) essentially forms the proposed feedback law that aims at compensating the pressure drop over the hose-filter system. Substituting the airway pressure, obtained from (6), into (12) gives

$$\Delta\hat{p} = \hat{R}_{\text{lin}}\left(C_{\text{lung}}\left(1+\frac{R_{\text{lung}}}{R_{\text{leak}}}\right)(\dot{p}_{\text{lung}} - \dot{p}_{\text{pat}}) + \frac{p_{\text{lung}}}{R_{\text{leak}}}\right). \tag{13}$$

For notational purposes, the combined variable

$$R(e_{\text{LS}}) := e_{\text{LS}}(R_{\text{leak}} + R_{\text{lung}}) + R_{\text{leak}} R_{\text{lung}} \tag{14}$$

is defined with the estimation error

$$e_{\text{LS}} := R_{\text{lin}} - \hat{R}_{\text{lin}}. \tag{15}$$

Then, substitution of (13) in (11) gives

$$\dot{p}_{\text{lung}} = \frac{-R_{\text{leak}} - e_{\text{LS}}}{C_{\text{lung}} R(e_{\text{LS}})} p_{\text{lung}} + \frac{R_{\text{leak}}}{C_{\text{lung}} R(e_{\text{LS}})} p_{\text{target}} + \dot{p}_{\text{pat}}. \tag{16}$$

The variables p_{aw}, Q_{pat}, and Q_{out} are considered as outputs, and the resulting closed-loop system is described as follows:

$$\begin{aligned}\dot{p}_{\text{lung}} &= \mathbf{A}(e_{\text{LS}}) p_{\text{lung}} + \mathbf{B}(e_{\text{LS}}) p_{\text{target}} + \dot{p}_{\text{pat}} \\ \begin{bmatrix} p_{\text{aw}} \\ Q_{\text{pat}} \\ Q_{\text{out}} \end{bmatrix} &= \mathbf{C}(e_{\text{LS}}) p_{\text{lung}} + \mathbf{D}(e_{\text{LS}}) p_{\text{target}}\end{aligned} \tag{17}$$

with

$$\begin{aligned}\mathbf{A}(e_{\text{LS}}) &= \frac{-R_{\text{leak}} - e_{\text{LS}}}{C_{\text{lung}} R(e_{\text{LS}})},\ \mathbf{B}(e_{\text{LS}}) = \frac{R_{\text{leak}}}{C_{\text{lung}} R(e_{\text{LS}})} \\ \mathbf{C}(e_{\text{LS}}) &= \begin{bmatrix} 1 - \dfrac{(R_{\text{leak}} + e_{\text{LS}}) R_{\text{lung}}}{R(e_{\text{LS}})} & \dfrac{-R_{\text{leak}} - e_{\text{LS}}}{R(e_{\text{LS}})} & \dfrac{-R_{\text{leak}}}{R(e_{\text{LS}})} \end{bmatrix}^T \\ \mathbf{D}(e_{\text{LS}}) &= \begin{bmatrix} \dfrac{R_{\text{leak}} R_{\text{lung}}}{R(e_{\text{LS}})} & \dfrac{R_{\text{leak}}}{R(e_{\text{LS}})} & \dfrac{R_{\text{leak}} + R_{\text{lung}}}{R(e_{\text{LS}})} \end{bmatrix}^T.\end{aligned} \tag{18}$$

Note that the dynamics in (17) are in fact nonlinear in the estimation error e_{LS} because of the dependence of the system matrices on this estimation error. Next, the system is analyzed for a constant least-squares estimation error e_{LS}. In particular, we are interested in these linear dynamics for $e_{\text{LS}} = 0$ to understand the closed-loop system behavior, with hose pressure compensation once a perfect hose resistance estimate is available. This analysis is performed by means of the transfer function of the linear system with a constant estimation error. From this transfer function, strong performance features of the closed-loop system are obtained.

Using the system dynamics in (17) and (18), the transfer function from the inputs p_{target} and $\dot{p}_{\text{pat}}$ to the output p_{aw} is computed. Hereto, the closed-loop system is rewritten in the following form:

$$\dot{p}_{\text{lung}} = \bar{\mathbf{A}} p_{\text{lung}} + \bar{\mathbf{B}} u \tag{19}$$

$$p_{\text{aw}} = \bar{\mathbf{C}} p_{\text{lung}} + \bar{\mathbf{D}} u \tag{20}$$

with a combined input vector $u = \begin{bmatrix} p_{\text{target}} & \dot{p}_{\text{pat}} \end{bmatrix}^T$

$$\bar{\mathbf{A}} = \mathbf{A}(e_{\text{LS}}), \quad \bar{\mathbf{B}} = \begin{bmatrix} \mathbf{B}(e_{\text{LS}}) 1 \end{bmatrix} \tag{21}$$

$$\bar{\mathbf{C}} = \mathbf{C}_1(e_{\text{LS}}), \quad \bar{\mathbf{D}} = \begin{bmatrix} \mathbf{D}_1(e_{\text{LS}}) 0 \end{bmatrix} \tag{22}$$

where $\mathbf{C}_1(e_{\text{LS}})$ and $\mathbf{D}_1(e_{\text{LS}})$ are the first elements in $\mathbf{C}(e_{\text{LS}})$ and $\mathbf{D}(e_{\text{LS}})$, respectively. Using this form of the closed-loop system, the transfer function from u to p_{aw} is obtained

$$\frac{p_{\text{aw}}(s)}{u(s)} = \bar{\mathbf{C}}(s - \bar{\mathbf{A}})^{-1}\bar{\mathbf{B}} + \bar{\mathbf{D}} \tag{23}$$

with $s \in \mathbb{C}$ the Laplace variable. Using this, an expression for p_{aw} is obtained

$$p_{\text{aw}}(s) = P_1 p_{\text{target}}(s) + P_2 \dot{p}_{\text{pat}}(s) \tag{24}$$

with

$$P_1 = \frac{R_{\text{leak}} + C_{\text{lung}} R_{\text{leak}} R_{\text{lung}} s}{R_{\text{leak}} + C_{\text{lung}} R_{\text{leak}} R_{\text{lung}} s + e_{\text{LS}}(1 + C_{\text{lung}}(R_{\text{leak}} + R_{\text{lung}}) s)}$$

and

$$P_2 = \frac{C_{\text{lung}} e_{\text{LS}} R_{\text{leak}}}{R_{\text{leak}} + C_{\text{lung}} R_{\text{leak}} R_{\text{lung}} s + e_{\text{LS}}(1 + C_{\text{lung}}(R_{\text{leak}} + R_{\text{lung}}) s)}.$$

Next, an exact estimate of the hose resistance is assumed, i.e., estimation error $e_{\text{LS}} = 0$. For an exact estimate of the hose resistance, the term P_1 in (24), i.e., the transfer function from p_{target} to p_{aw}, is one for all $s \in \mathbb{C}$. Furthermore, the term P_2, i.e., the transfer function from $\dot{p}_{\text{pat}}$ to p_{aw},

is zero for all $s \in \mathbb{C}$. Therefore, the airway pressure of the closed-loop system is exactly the same as p_{target}. Furthermore, the airway pressure is independent of the patient dynamics and the exogenous disturbance $\dot{p}_{\text{pat}}$ related to the patient effort. This is a highly desirable property for a controlled system. A formal proof of these properties (zero tracking error independent of patient effort and patient dynamics) for the full nonlinear dynamics, i.e., with convergence of e_{LS} to zero, is presented in Section IV-C.

B. RLS Estimation of the Hose Resistance

In Section IV-A, the equations describing the proposed controlled plant model are presented for a given (constant) hose resistance estimate $\hat{R}_{\text{lin}}$. Since the hose resistance is an unknown parameter, an RLS estimator that estimates the value of R_{lin} automatically during ventilation is proposed; hence, no additional calibration steps are required in the hospital. In this particular application, an RLS algorithm with exponential forgetting factor β is used [17, p. 200], since data far in the past is considered less important than more recent data. A schematic of the system, including the hose resistance estimator, is shown in Fig. 4.

The RLS estimator with forgetting factor is given by[1]:

$$\dot{\hat{R}}_{\text{lin}} = P\frac{\Delta p - \hat{R}_{\text{lin}} Q_{\text{out}}}{m^2} Q_{\text{out}} \tag{25}$$

$$\dot{P} = \beta P - P^2 \frac{Q_{\text{out}}^2}{m^2} \tag{26}$$

where Q_{out} is the exciting variable, $P(t)$ is called the covariance, and $(\Delta p - \hat{R}_{\text{lin}} Q_{\text{out}})/(m^2)$ represents the normalized estimation error of the pressure drop, with $m^2 > 0$ a constant normalization parameter. Since $\Delta p = R_{\text{lin}} Q_{\text{out}}$, $e_{\text{LS}}(t) = R_{\text{lin}} - \hat{R}_{\text{lin}}(t)$, and R_{lin} is a constant, the least-squares error dynamics are written as follows:

$$\dot{e}_{\text{LS}} = -P\frac{Q_{\text{out}}^2}{m^2} e_{\text{LS}}. \tag{27}$$

The resulting closed-loop dynamics with estimator and hose compensation controller are given by (17), (18), (26), and (27).

The parameters β and $P(0)$ should be chosen such that convergence is sufficiently fast, i.e., within a couple of breaths. However, choosing β too high results in fast convergence but might also result in strong oscillations in the parameter due to the measurement noise and effects that are not captured by the hose model. Furthermore, β and $P(0)$ should be positive to ensure stability as discussed in Section IV-C. In addition, in this article, the constant normalization parameter m is chosen to be one, i.e., $m = 1$, to reduce the number of tuning parameters.

C. Stability Analysis

The closed-loop system dynamics with the adaptive controller are given by (17), (18), (26), and (27). In this section, stability conditions for the closed-loop controlled system are derived. First, several auxiliary results are presented. Using these auxiliary results, Theorem 1 is presented in the following. Theorem 1 provides sufficient conditions for exponential convergence to zero of the tracking error $e(t)$ and of the estimation error $e_{\text{LS}}(t)$. Herein, we consider time-varying pressure targets $p_{\text{target}}(t)$, unknown patient effort $p_{\text{pat}}(t)$, and unknown patient-hose parameters, i.e., resistances and compliance. In support of the proofs, the auxiliary lemmas in the Appendix are used.

First, a Persistently Exciting (PE) signal is defined.

Definition 1: A piecewise continuous scalar signal $\phi(t)$ is PE if there exist constants $\alpha_0, \alpha_1, T_0 \in \mathbb{R}_{>0}$ such that

$$\alpha_1 \geq \frac{1}{T_0}\int_t^{t+T_0} \phi^2(\tau) d\tau \geq \alpha_0 \quad \forall t \geq 0. \tag{28}$$

Furthermore, the RLS estimator in (26) and (27) is assumed to satisfy Assumption 1.

Assumption 1: The RLS estimator in (26) and (27) is designed and initialized such that the following properties hold.

1) $P(0)$ is chosen to be positive, i.e., $P(0) > 0$.
2) $\hat{R}_{\text{lin}}(0)$ is chosen such that the following inequalities hold (with $\epsilon > 0$ a small constant):

$$\hat{R}_{\text{lin}}(0) < R_{\text{lin}} + R_{\text{leak}}$$
$$\hat{R}_{\text{lin}}(0) \leq R_{\text{lin}} + \frac{R_{\text{leak}} R_{\text{lung}}}{R_{\text{leak}} + R_{\text{lung}}} - \epsilon.$$

3) β is designed to be positive, i.e., $\beta > 0$.

Note that we can always design and initialize the RLS estimator such that Assumption 1 holds. Furthermore, choosing $\hat{R}_{\text{lin}}(0) = 0$ directly ensures the inequalities in Assumption 1 since all resistances are positive, though this may be a conservative initial estimate for the hose resistance.

Assumption 2 states that the target pressure profile is always positive and bounded.

Assumption 2: $p_{\text{target}}(t)$ is bounded and positive by design; in particular, $\epsilon_1 < p_{\text{target}}(t) < \infty$, $\forall t \geq 0$, with $\epsilon_1 > 0$ a positive constant.

This is a valid assumption since a positive and bounded target pressure is desired during positive pressure ventilation (see Fig. 2), with PEEP > 0.

Assumption 3 states that the disturbance $\dot{p}_{\text{pat}}(t)$ is bounded.

Assumption 3: The patient effort $p_{\text{pat}}(t)$ is a bounded signal. Furthermore, its time derivative $\dot{p}_{\text{pat}}(t)$ is a bounded signal as well.

Assumption 3 is valid in practice since a patient cannot generate unbounded pressure or derivatives in pressure.

Note that PE conditions on the excitation signals are required to guarantee the RLS estimators with a forgetting factor to converge (see [17, Corollary 4.3.2]). Here, the exciting variable $Q_{\text{out}}(p_{\text{lung}}(t), e_{\text{LS}}(t), p_{\text{target}}(t))$ is not an external signal, but a variable dependent on the states [see (17), (18)]. This complicates the stability analysis and requires an analysis of the PE properties of $Q_{\text{out}}(p_{\text{lung}}(t), e_{\text{LS}}(t), p_{\text{target}}(t))$ as in Lemma 1. Note that no additional excitations are induced to ensure the PE condition, i.e., Q_{out} is PE in the considered, common, ventilation scenarios.

Lemma 1: Consider the closed-loop system dynamics defined by (17), (18), (26), and (27) and adopt

[1]The notation equivalents to the notation of [17, p. 200] are $R_{\text{lin}} = \theta^*$, $\hat{R}_{\text{lin}} = \theta$, $Q_{\text{out}} = \phi_0$, and $\Delta p = z$.

Assumptions 1–3. Then, $Q_{\text{out}}(p_{\text{lung}}(t), e_{\text{LS}}(t), p_{\text{target}}(t))$ is PE as defined in Definition 1.

Proof: To ensure the existence of upper bound α_1 of the PE condition in Definition 1, Lemma 5 in the Appendix is invoked, which ensures that $Q_{\text{out}}(p_{\text{lung}}(t), e_{\text{LS}}(t), p_{\text{target}}(t))$ is bounded for all $t \geq 0$. Since $Q_{\text{out}}(p_{\text{lung}}(t), e_{\text{LS}}(t), p_{\text{target}}(t))$ is bounded, $\alpha_1 > 0$ indeed exists such that the upper bound in (28) is satisfied for $\phi(t) := Q_{\text{out}}(p_{\text{lung}}(t), e_{\text{LS}}(t), p_{\text{target}}(t))$.

Next, we have to show that the lower bound α_0 in the PE condition in (28) exists. For such lower bound to exist, the following equality should not hold for any $t^* \geq 0$ for some $T_0 \in \mathbb{R}_{>0}$:

$$Q_{\text{out}}(p_{\text{lung}}(t), e_{\text{LS}}(t), p_{\text{target}}(t)) = 0 \quad \forall t \in [t^*, t^* + T_0]. \tag{29}$$

If there is no output flow, i.e., $Q_{\text{out}}(p_{\text{lung}}(t), e_{\text{LS}}(t), p_{\text{target}}(t)) = 0$, then from (2), $-Q_{\text{leak}} = Q_{\text{pat}}$. Furthermore, the pressure drop $p_{\text{aw}} - p_{\text{out}} = \Delta p = R_{\text{lin}} Q_{\text{out}}$ and the estimated pressure drop $\Delta \hat{p} = \hat{R}_{\text{lin}} Q_{\text{out}}$ are also zero under such condition. Using this and Assumption 2 gives $p_{\text{aw}}(t) = p_{\text{out}}(t) = p_{\text{target}}(t) > \epsilon_1 \, \forall t \in [t^*, t^* + T_0]$ if $Q_{\text{out}}(p_{\text{lung}}(t), e_{\text{LS}}(t), p_{\text{target}}(t)) = 0 \, \forall t \in [t^*, t^* + T_0]$. Moreover, $-Q_{\text{leak}} = Q_{\text{pat}}$ in combination with (3) gives

$$-\frac{p_{\text{target}}}{R_{\text{leak}}} = \frac{p_{\text{target}} - p_{\text{lung}}}{R_{\text{lung}}} \tag{30}$$

which is rewritten to obtain

$$p_{\text{lung}}(t) = \frac{R_{\text{lung}}}{R_{\text{leak}}} p_{\text{target}}(t) + p_{\text{target}}(t) \quad \forall t \in [t^*, t^* + T_0]. \tag{31}$$

Using (4) and (31), we obtain

$$\frac{1}{C_{\text{lung}}} \int_{t^*}^{t} Q_{\text{pat}}(\tau) d\tau + p_{\text{pat}}(t) + p_{\text{lung}}(t^*) = \frac{R_{\text{lung}}}{R_{\text{leak}}} p_{\text{target}}(t) + p_{\text{target}}(t) \quad \forall t \in [t^*, t^* + T_0]$$

which is rewritten to

$$-\frac{1}{C_{\text{lung}} R_{\text{leak}}} \int_{t^*}^{t} p_{\text{target}}(\tau) d\tau + p_{\text{pat}}(t) + p_{\text{lung}}(t^*) = \frac{R_{\text{lung}}}{R_{\text{leak}}} p_{\text{target}}(t) + p_{\text{target}}(t) \quad \forall t \in [t^*, t^* + T_0] \tag{32}$$

using $Q_{\text{pat}} = -(p_{\text{target}}/R_{\text{leak}})$. We can choose a value $T_0 \in \mathbb{R}_{>0}$ such that this will not hold for any $t^* \geq 0$. If we take $T_0 \to \infty$, the term with the integral will go to minus infinity, using Assumption 2. We know that $p_{\text{pat}}(t)$ and $p_{\text{lung}}(t^*)$ are bounded using Assumption 3 and Lemma 4, respectively. Hence, the left-hand side of the equation will become negative for large values of T_0 and the right-hand side is always positive by Assumption 2. Since (32) does not hold for $T_0 \to \infty$, we know that (29) does not hold for any t^* for some very large T_0. Therefore, we can conclude that $Q_{\text{out}}(p_{\text{lung}}(t), e_{\text{LS}}(t), p_{\text{target}}(t))$ is PE, according to Definition 1. □

Finally, using Lemma 1 and Lemmas 4 and 5 in the Appendix, the stability of the closed-loop system, including the RLS estimator is proven. More precisely, Theorem 1 shows the exponential convergence of the least-squares error $e_{\text{LS}}(t)$ and the tracking error $e(t)$ to zero.

Theorem 1: Consider the system dynamics (17), (18), (26), and (27) and suppose that Assumptions 1, 2, and 3 hold. Then, solutions of the dynamical system (17), (18), (26), and (27) have the following properties.

1) $P(t)$, $P^{-1}(t)$, $p_{\text{lung}}(t)$, and $Q_{\text{out}}(t)$ are bounded $\forall t \geq 0$.
2) $e_{\text{LS}}(t) = R_{\text{lin}} - \hat{R}_{\text{lin}}(t)$ and $e(t) = p_{\text{target}}(t) - p_{\text{aw}}(t)$ exponentially converge to zero.

Proof: First of all, the boundedness of p_{lung} and Q_{out} is shown in Lemmas 4 and 5, respectively (see the Appendix). Furthermore, using Lemma 2, we know that $P(t)$ and $P^{-1}(t)$ are bounded $\forall t \geq 0$.

From Lemma 1, we know that the PE property holds for $Q_{\text{out}}(t)$. Therefore, [17, Corollary 4.3.2] can be used to show that $e_{\text{LS}}(t)$ is exponentially converging to zero.

Finally, we have to show that $e(t)$ exponentially converges to zero. By substituting the airway pressure p_{aw}, defined in (17) and (18), into the error definition $e(t)$, defined in (1), the tracking error can be written as

$$\begin{aligned} e(t) &= \frac{-R_{\text{leak}} p_{\text{lung}}(t) + (R_{\text{leak}} + R_{\text{lung}}) p_{\text{target}}(t)}{e_{\text{LS}}(t)(R_{\text{leak}} + R_{\text{lung}}) + R_{\text{leak}} R_{\text{lung}}} e_{\text{LS}}(t) \\ &=: \upsilon(t) e_{\text{LS}}(t). \end{aligned} \tag{33}$$

Since, first, $p_{\text{lung}}(t)$ is bounded (Lemma 4), second $p_{\text{target}}(t)$ is bounded (Assumption 2), and third, $e_{\text{LS}}(R_{\text{leak}} + R_{\text{lung}}) + R_{\text{leak}} R_{\text{lung}}$ is bounded away from zero (as shown in Lemma 4), it is guaranteed that $\upsilon(t)$ in (33) is bounded. Since $\upsilon(t)$ is bounded $\forall t \geq 0$, i.e., there exists a bounded $\upsilon_{\max}$, such that $|\upsilon(t)| \leq \upsilon_{\max} \forall t \geq 0$, we can write

$$|e(t)| \leq \upsilon_{\max} |e_{\text{LS}}(t)| \quad \forall t > 0. \tag{34}$$

Since $e_{\text{LS}}(t)$ converges to zero exponentially, (34) shows that $e(t)$ also converges to zero exponentially. □

Theorem 1 ensures exponential convergence of the tracking error $e(t)$ to zero for a time-varying target pressure, under mild conditions on the initial estimate for the hose resistance and the target pressure profile $p_{\text{target}}(t)$. Furthermore, this property is independent of the unknown disturbance induced by the patient's breathing effort, as long as it remains bounded. In control systems, perfect tracking is typically possible when inverse-plant feedforward is applied and no further disturbances are present. In this case, it is achieved by compensating for the disturbance through feedback. More precisely, the measured flow Q_{out} that is used in the feedback loop contains the disturbance, i.e., Q_{out} depends on $\dot{p}_{\text{pat}}$ through p_{lung}. The estimate of the hose resistance is used to compensate for the pressure drop such the target pressure is an invariant solution of the closed-loop dynamics. This can be seen in (24) with $e_{\text{LS}} = 0$, which gives $p_{\text{aw}} = p_{\text{target}}$ independent of the patient effort and dynamics. This is achieved independent of the system, i.e., patient and hose, parameters as mentioned in Remark 1. The system parameters only affect the flow and therewith the convergence speed of the hose-resistance estimate.

Remark 1: The relation between the hose-induced pressure drop Δp and the measured flow through the hose Q_{out} is independent of the patient and leak parameters, and the patient effort. The patient and leak parameters only influence the measured blower output flow Q_{out}, and therewith, the convergence

TABLE I

ESTIMATION PARAMETERS OF THE ADAPTIVE CONTROLLER AND THE PATIENT AND HOSE PARAMETERS AS USED IN THE SIMULATIONS

Parameter	Value	Unit
β	0.7	1/s
$P(0)$	5×10^{-8}	s/mL^2
$\hat{R}_{lin}(0)$	0	mbar s/L
m	1	-
R_{leak}	24	mbar s/L
R_{lung}	5	mbar s/L
$R_{lin}(0)$	4.4	mbar s/L
C_{lung}	20	mL/mbar

speed of the estimator is affected. However, exact tracking of the target pressure independent of patient and leak parameters and the patient effort is achieved.

V. SIMULATION CASE STUDY

In this section, the improvement in tracking performance of the proposed adaptive control approach compared to state-of-practice control strategies is shown through simulations. The performance of the different control strategies is compared by analyzing the pressure tracking, i.e., rise time, overshoot, undershoot, and settling time. Furthermore, overshoot in patient flow is considered since a decrease in overshoot prevents false triggering and improves patient comfort.

Two different scenarios are considered is this section. In Section V-A, a sedated patients, i.e., $p_{\text{pat}}(t) = 0\,\forall t$, under PCV ventilation is considered. In Section V-B, a spontaneously breathing patient, i.e., $\exists t \geq 0 : p_{\text{pat}}(t) \neq 0$, under CPAP ventilation is considered.

In the case with a sedated patient, a step in the hose resistance is introduced to show that the new control approach can handle changes in resistance, which may be induced by clogging of a filter. The following two state-of-practice control strategies are considered to benchmark against feedforward control and linear feedback control.

The feedforward controller is a unit feedforward; in other words, the desired airway pressure is applied as $p_{\text{target}} = p_{\text{control}} = p_{\text{out}}$ and no feedback based on measurements is used. For the linear feedback controller, an integral controller is used to compensate for the pressure drop Δp over the hose. This feedback controller is used in addition to the unit feedforward controller. The integral controller results in the convergence of the tracking error to zero for constant target pressures. Because the plant variations are large, the linear feedback controller is tuned for robustness instead of performance resulting in an integral controller with transfer function $C(s) = (10/s)$, with $s \in \mathbb{C}$ the Laplace variable. The RLS estimator parameters and the patient-hose system parameters are presented in Table I.

A. Scenario With Sedated Patients

First of all, the ventilation of sedated patients under PCV is considered. This section is divided into the test case description, the simulation results, and a summary of the main conclusions.

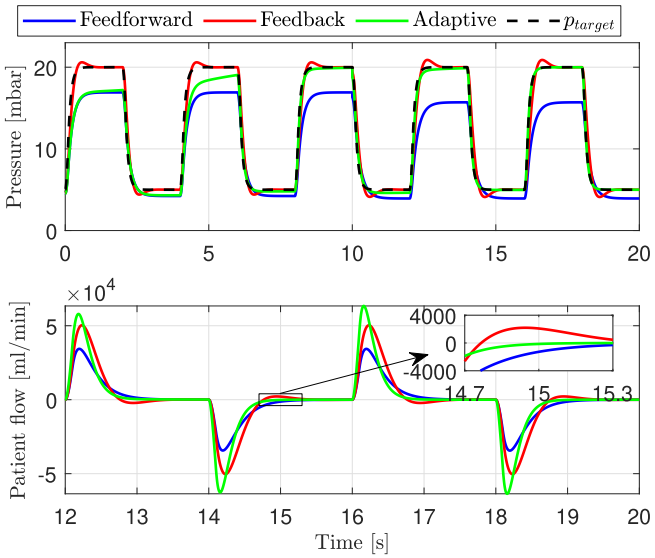

Fig. 6. Simulation results of the feedforward, feedback, and adaptive control strategy. This shows the resulting airway pressure and patient flow.

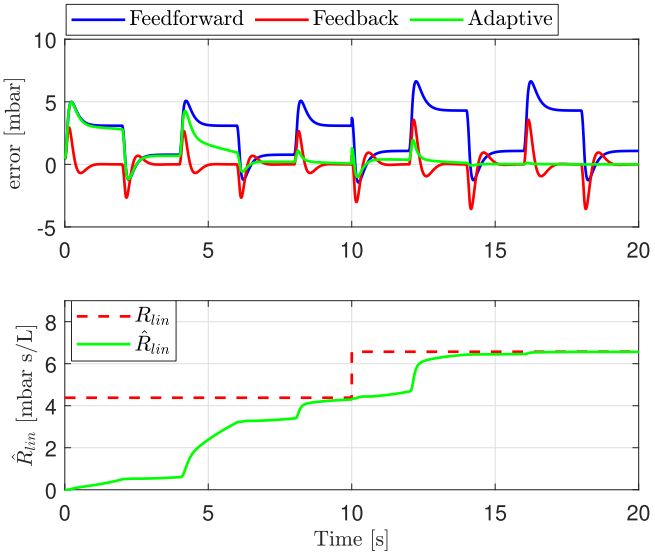

Fig. 7. Tracking errors of the different controllers and convergence of $\hat{R}_{\text{lin}}$ of the adaptive controller.

1) Test Case: In these simulations, the target pressures of 5 and 20 mbar are used for the PEEP and the IPAP, respectively. Furthermore, we introduce a step in the hose resistance at $t = 10$ s, to show that the controller can handle a change in resistance. This step in resistance is shown in the bottom of Fig. 7. Finally, simulations with different patient characteristics, such as compliance and resistance, are performed to show that the controller works for a wide range of patients.

2) Simulation Results: The resulting airway pressure of the simulations is shown in Fig. 6. These results clearly show that the feedforward controlled system has a steady-state tracking error, which is caused by the pressure drop Δp over the hose. For the linear feedback controller it is observed that the pressure is converging to the desired pressure, but there is

undesired overshoot and undershoot caused by the feedback controller. This results in nonoptimal patient support. More specifically, the undershoot in pressure causes overshoot in the patient flow, see the zoomed inset in the bottom of Fig. 6. Overshoot in patient flow may result in false triggers during ventilation modes that allow for patient-triggered breaths (see [6]). The resulting airway pressure of the developed adaptive controller is also shown in Fig. 6. It shows that during the first breathing cycle, the proposed controller behaves almost the same as the feedforward controller. This is caused by the initial estimate of $\hat{R}_{\text{lin}}(0) = 0$, resulting in $\Delta\hat{p} \approx 0$ during the first breath, i.e., the adaptive controller is not compensating the pressure drop yet. In the third breathing cycle, almost perfect tracking with no overshoot and oscillations is achieved. Thereafter, at $t = 10$ s, the controller has to adapt to the step in R_{lin}, which introduces a deviation between the target pressure p_{target} and the airway pressure p_{aw}. This has almost completely vanished after the fifth breathing cycle.

In Fig. 7, the significant improvement in tracking performance is visualized. The tracking error of the adaptive controller indeed converges to zero. The tracking errors of the feedforward and feedback controllers remain the same over successive breaths, with a slight increase when the hose resistance is increased. Furthermore, Fig. 7 shows that the estimated resistance is converging to the actual value as expected. Therefore, no manual calibration of the hose is required such that no additional time of the hospital staff is required. It is also clearly observed that the controller can handle the step in hose resistance since the tracking error is converging to zero again after the step in resistance.

The convergence of the estimator takes about 10 s, i.e., 2–3 breaths. In practice, this is sufficiently fast because a patient breaths over 20 000 times a day. Therefore, these three breaths are considered negligible in practice. Furthermore, a manual calibration typically takes longer, during which the patient is not ventilated at all. Therefore, the adaptive scheme is preferred over a manual calibration procedure.

Pressure profiles for different lung characteristics (resistance and compliance, see legend) are shown in Fig. 8. This figure shows that the control approach works for a broad range of patients. The patient parameters do affect the flow and, therewith, the estimator performance is slightly affected. However, the estimator will converge and the compensation ultimately achieves perfect tracking independent of the patient parameters.

3) Main Conclusion: The simulations show that the estimation error $e_{\text{LS}}(t)$ converges to zero and, therewith, the tracking error $e(t)$ converges to zero as well, as expected from Section IV-C. Furthermore, the simulations show that there is no overshoot in patient flow, preventing false triggering of breaths. It is also shown that the adaptive controller works for a broad range of patients and is able to handle changes in the hose resistance.

B. Scenario With Spontaneously Breathing Patients

Since many patients are conscious and, therewith, able to breathe themselves, another common ventilation mode is considered, namely, CPAP. CPAP aims to maintain a constant positive airway pressure to assist the patient's breathing and to keep the lungs open. Also, this section is divided into the test case description, the simulation results, and a summary of the main conclusions.

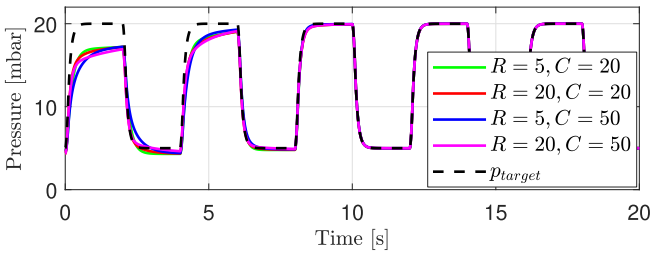

Fig. 8. Airway pressure p_{aw} for multiple types of lungs, with the adaptive controller. The lung characteristics are given in the legend where the units for R are mbar s/L and the units for C are mL/mbar.

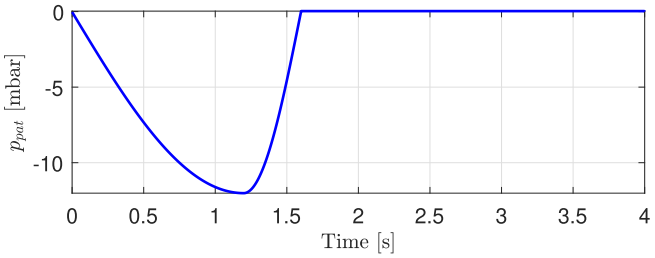

Fig. 9. Plot of the patient effort of the spontaneously breathing patient. This patient effort is used in the simulations and experiments.

1) Test Case: The considered patient has a respiratory rate of 15 breaths per minute and generates a pressure of -12 mbar in the lungs. The patient effort profile is a semisinusoidal profile, similar to semisinusoidal profile of the ASL 5000 Breathing Simulator, which is used in the experiments in Section VI. The patient effort curve is shown in Fig. 9. Note that there is no consensus on how to model realistic patient effort according to [18]. However, the default semisinusoidal of the ASL 5000 Breathing Simulator is most often used according to [19]. The target pressure used in this simulation is 5 mbar. Furthermore, we used the same control and patient-hose parameters as in Section V-A (see Table I).

2) Simulation Results: The resulting airway pressure p_{aw} for the feedforward, feedback, and adaptive controller is shown in Fig. 10. It is clearly shown that the airway pressure converges to the desired constant pressure with the adaptive controller. In the other two control approaches, we observe the undesired pressure oscillations, caused by the patient's effort, around the pressure target. This case study shows that the developed adaptive controller improves the tracking performance significantly during CPAP ventilation.

3) Main Conclusion: These simulations show that the tracking performance is improved (see Fig 10). The adaptive controller achieves exact tracking of the desired airway pressure, whereas the feedforward and feedback controller show significant spikes in the airway pressure, caused by the patient's effort.

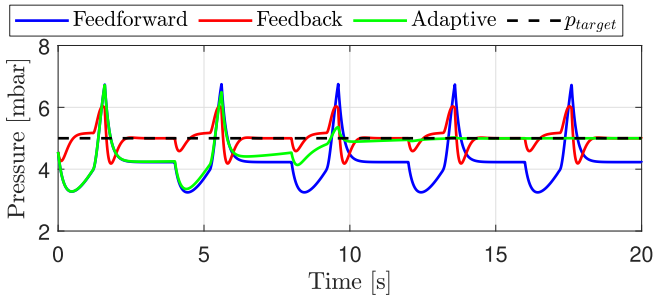

Fig. 10. Simulation results of the feedforward, feedback, and adaptive control strategy. This shows the resulting airway pressure of a spontaneously breathing patient with the CPAP ventilation mode.

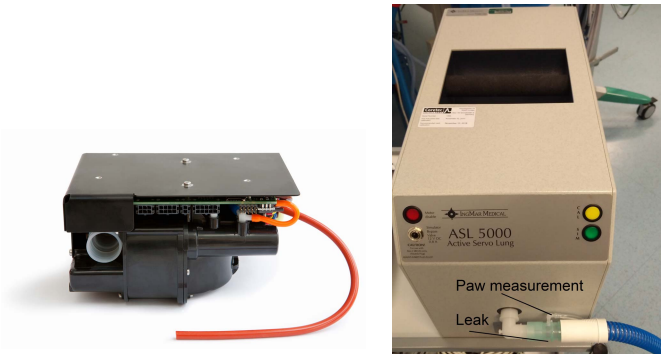

(a) (b)

Fig. 11. Main components of the experimental setup. (a) Macawi blower-driven mechanical Ventilator. (b) ASL 5000 breathing simulator.

VI. Experimental Case Study

In order to show the practical applicability and performance of the adaptive controller, an experimental case study has been conducted. First of all, the results of two experiments for the scenario of a fully sedated patient on PCV are shown. Thereafter, the results for the scenario of a spontaneously breathing patient with CPAP ventilation are presented.

The main components of the experimental setup used in this case study are shown in Fig. 11. In Fig. 11(a), a blower-driven mechanical ventilation module of Macawi is shown [20]. Inside this module, the commercially available Macawi respiratory centrifugal blower with its custom motor and motor controller is used for the actuation of the system [20]. The blower flow Q_{out} is measured using a MEMS thermal flow sensor inside the respiratory module. Both the airway pressure p_{aw} and the blower outlet pressure p_{out} are measured using a gauge pressure sensor inside the respiratory module. The ventilator is attached to a dSPACE system (dSPACE GmbH, Paderborn, Germany), where the controls are implemented using MATLAB Simulink (MathWorks, Natick, MA, USA) running at a sampling frequency of 500 Hz.

Furthermore, the ASL 5000 Breathing Simulator (IngMar Medical, Pittsburgh, PA, USA), as shown in Fig. 11(b), is used to emulate the patient. This lung simulator can be used to emulate a wide variety of patients with a linear resistance and compliance. Furthermore, it is able to simulate a patient with breathing effort.

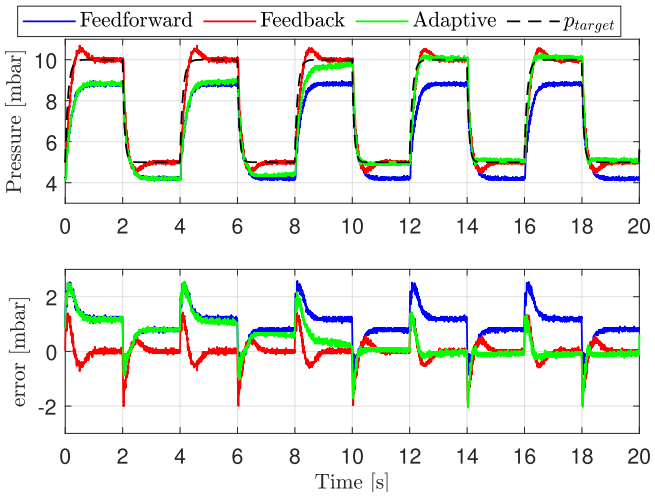

Fig. 12. Experimental results of the feedforward, feedback, and adaptive control strategy. This shows the resulting airway pressure and tracking error of the different controllers with a target pressure of PEEP and IPAP of 5 and 10 mbar, respectively.

The patient and controller parameters in the experiments are the same as the corresponding parameters in the simulations of Section V (see Table I). However, the hose and leak resistance in the simulations are estimated using an offline least-squares fit of the actual hose resistance, and this results in a slight parametric difference between the simulation and experimental scenarios.

A. Scenario With Sedated Patients

In this section, the ventilation of a sedated patient under PCV is considered. This section is divided into the test case description, experimental results, and a summary of the main conclusions.

1) Test Case: The same patient and controller parameters as in the simulation case study for sedated patients are used (Table I). Furthermore, two different target profiles are considered. First of all, a target profile is used with a PEEP and IPAP of 5 and 10 mbar, respectively. This first test case, with low pressures, is considered to validate the developed control strategy and its theory. These low pressures result in low flows, and hence, the linear component of the hose resistance is dominant over the quadratic part. Thereafter, the same target profile as in the simulation case study is used with a PEEP and IPAP of 5 and 20 mbar, respectively. Another difference with the simulation-based case study is that the hose resistance in the experiments is constant. In other words, the experiments do not contain a step in the hose resistance.

2) Experimental Results: First of all, the results of the experiments with the IPAP of 10 mbar are presented and discussed. Thereafter, the results of the experiments with the IPAP of 20 mbar are shown and discussed.

The results of the experiments with the IPAP of 10 mbar are shown in Figs. 12 and 13. The airway pressure and tracking error $e = p_{\text{target}} - p_{\text{aw}}$ are depicted in Figs. 12 and 13. Figs. 12 and 13 clearly show the constant offset in the airway pressure for the unit feedforward controller. Furthermore, it is

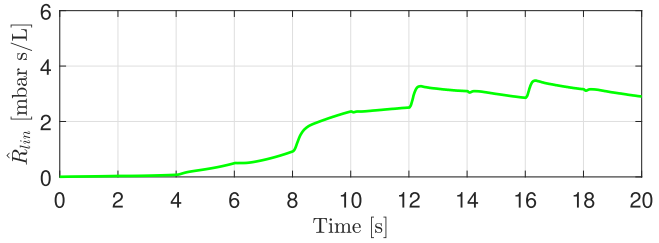

Fig. 13. Experimentally obtained estimate of the hose resistance for a target pressure of PEEP and IPAP of 5 and 10 mbar, respectively.

clearly shown that the feedback controller has significant overshoot and undershoot. As expected, the adaptive controller converges after approximately three breaths (see Fig. 13). The resistance estimate is slightly oscillating upon convergence, and this is caused by the quadratic nature of the hose resistance. However, these oscillations are considered small because the outlet flow Q_{out} remains in a small interval. Fig. 12 shows that upon convergence, the adaptive controller achieves a significantly better tracking performance than the feedforward controller. Furthermore, the adaptive controller shows significantly less overshoot and undershoot than the linear feedback controller. These overshoots are undesired because the resulting peak pressures might damage the lungs. Furthermore, the undershoot is undesired since it causes oscillations in the patient flow, possibly resulting in false triggering. Considering the tracking error in the bottom of Fig. 12, it is noticed that still sharp peaks are present during the increase and decrease of the pressure for both feedback control strategies. These peaks are mainly caused by a delay in the blower transfer from p_{control} to p_{out} and the measurement delay of the airway pressure p_{aw}. The blower delay causes a timing mismatch between the desired controller pressure p_{control} and the blower outlet pressure p_{out}. Furthermore, the measurement delay of the airway pressure p_{aw} causes a timing mismatch between the performance variable p_{aw} and the target pressure p_{target}. This measurement delay is clearly visible in the tracking error during changes of p_{target}.

The results of the experiments with the IPAP of 20 mbar are shown in Figs. 14 and 15. The obtained response is similar to the simulations for both the feedback and the feedforward controller. The feedforward controller does not compensate for the pressure drop over the hose. The feedback controller shows overshoot and undershoot in airway pressure p_{aw}. This causes overshoot in the patient flow, which might cause false triggering in triggered ventilation modes. Hence, such overshoots are highly undesired.

The adaptive controller shows the convergence of the airway pressure during the first few strokes. Thereafter, a clear decrease in overshoot and undershoot compared to the linear feedback controller is seen. The reduction in overshoot prevents ventilator-induced lung injury caused by peak pressures. Furthermore, the reduction in undershoot is beneficial in preventing oscillations in the patient flow. These oscillations are unpleasant for the patient and might result in false ventilator-induced triggering. Therefore, the adaptive

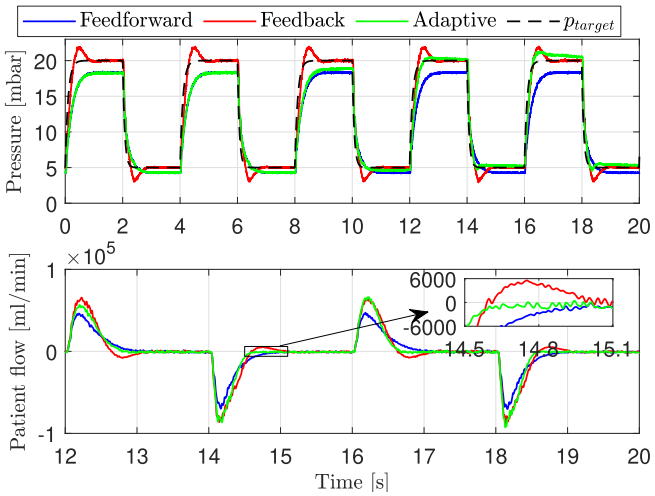

Fig. 14. Experimental results of the feedforward, feedback, and adaptive control strategy. This shows the resulting airway pressure and patient flow with a target pressure of PEEP and IPAP of 5 and 20 mbar, respectively.

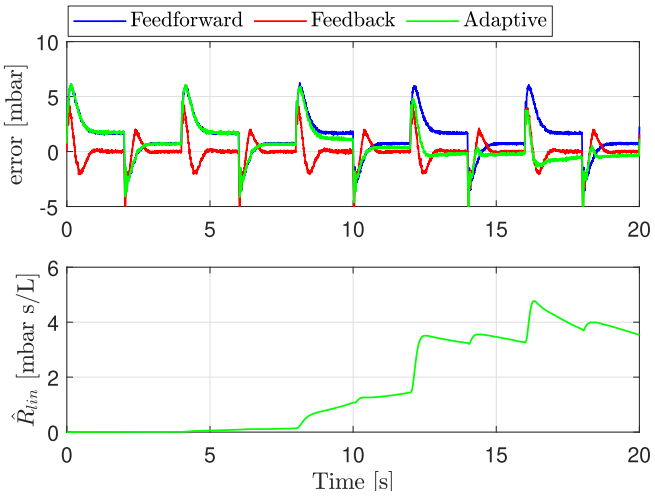

Fig. 15. Tracking errors of the different controllers and convergence of $\hat{R}_{\text{lin}}$ of the adaptive controller with a target pressure of PEEP and IPAP of 5 and 20 mbar, respectively.

controller improves patient comfort and consistency of the treatment. Besides all these improvements, during the fifth breath, the adaptive controller is slightly overcompensating the pressure drop, causing overshoot in the airway pressure (see Fig. 14). This is explained by the fact that a linear resistance model is used to estimate the quadratic hose resistance of the actual hose. This causes the estimator to overestimate the resistance during the start of inhalation. The high flows during inhalation result in a large contribution of the quadratic term to the pressure drop. When the flow has converged to a steady value during the remainder of the inhalation, the controller will overcompensate the pressure drop, causing the pressure to exceed the IPAP level. This oscillation of the estimated resistance is clearly shown in Fig. 15.

A visualization of the resistance estimate $\hat{R}_{\text{lin}}$ compared to the actual resistance is shown in Fig. 16. Fig. 16 also shows the pressure drop Δp over the hose on the left vertical axis

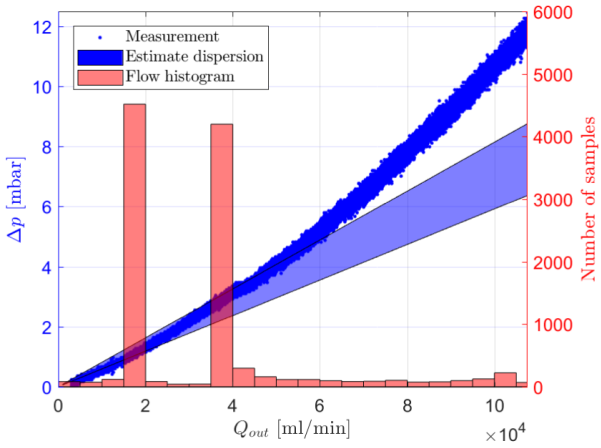

Fig. 16. Variation of the estimated hose model, linear resistance with estimated $\hat{R}_{\text{lin}}$, with the actual measured model with a target pressure of PEEP and IPAP of 5 and 20 mbar, respectively. Maximum flow in this figure is the same as the maximum flow Q_{out} through the hose in the experiment.

and the flow through the hose Q_{out} on the horizontal axis. The estimated resistance model, i.e., after 16 s in Fig. 15, is depicted by the blue area, and the estimated resistance model is oscillating in this area. The blue dots show the actual measured resistance model of the hose. This shows that the estimate is still fairly accurate in the low outlet flow area, up to 4×10^4 mL/min. The histogram in Fig. 16 displays how often a given flow is measured. Since the flow is mainly in the low flow regime, the linear estimate is fairly accurate on average.

3) Main Conclusion: This experimental study shows that the adaptive controller is practically applicable to sedated patients under PCV. The experimental study with low flows shows that the tracking error converges to zero and decreases overshoot and undershoot significantly compared to the linear feedback controller. The error is clearly converging to zero except for the region where the pressure is increasing and decreasing. In these areas, the controller is responding slightly too late, which is mainly caused by the presence of delays in the system. In the experimental case study with higher pressures and flows, the tracking error decreased significantly compared to the state-of-practice controllers. In particular, the adaptive controller prevents overshoot in patient flow, which prevents false triggering. It should be noted that performance could be further improved by using a quadratic resistance model in the adaptive controller; this could prevent oscillations of the resistance estimate. Furthermore, it may improve the accuracy of the estimated pressure drop and therewith the tracking performance. To improve the performance even further, the delays in the system should be analyzed and compensated in the control strategy. The latter two aspects are considered outside the scope of this article.

B. Scenario With Spontaneously Breathing Patients

In this section, the results of an experiment with a spontaneously breathing patient under CPAP ventilation are presented and discussed. Again, the section is divided into the test case description, experimental results, and a summary of the main conclusion.

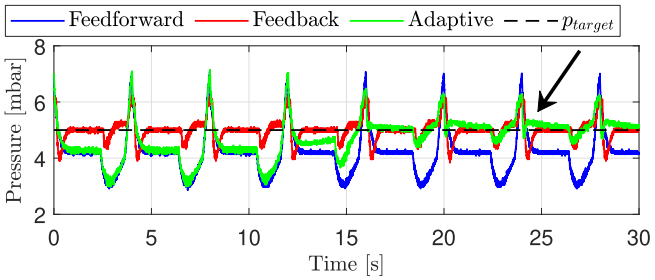

Fig. 17. Experimental results of the feedforward, feedback, and adaptive control strategy. This shows the resulting airway pressure of a spontaneously breathing patient with the CPAP ventilation mode.

1) Test Case: The same setup, i.e., patient, hose, leak, and controllers, is used as in the previous experiments. Furthermore, the patient effort is the same as in the simulations and is shown in Fig. 9. This profile is generated by the ASL 5000 Breathing Simulator, which is used in the experiments. The target pressure used in this simulation is 5 mbar.

2) Experimental Results: The resulting airway pressure for all three controllers is shown in Fig. 17. The feedforward and feedback controller show the results comparable to the simulations. The adaptive controller shows an improvement in tracking performance. The biggest improvement is the decrease in undershoot (see the arrow in Fig. 17). Furthermore, the same problem as for the fully sedated patient is seen; the controller is slightly overestimating the resistance during inhalation. This causes the pressure to be slightly higher than desired after inhalation and it is slowly converging to the desired value (see Fig. 17). Furthermore, Fig. 17 shows some peaks when the patient starts and ends inhalation, and this indicates that the controller does not respond fast enough to the patient-induced disturbance.

3) Main Conclusion: This experimental case study shows that the adaptive controller is practically applicable to spontaneously breathing patients as well. The overall performance is improved over the state-of-practice controllers. However, it shows the oscillations in the patient airway pressure p_{aw}, whereas the simulations showed exact convergence.

In conclusion, the adaptive controller shows an overall improvement in performance over the state-of-practice controllers. However, the performance of the adaptive controller could be further improved by using a more realistic hose model, i.e., including a quadratic term. Another problem that affects the performance in experiments is the delay in the sensor line of the airway pressure. This delay causes a timing mismatch between the measured signals. Compensation for this delay in the estimator might improve performance as well.

VII. Conclusion

In this article, an adaptive control approach for mechanical ventilation is presented. This control approach aims to improve the tracking performance for large variations of patient-hose parameters, unintended leakages, and unknown patient breathing efforts. It has been shown through stability analysis that this controller ensures the exact tracking of the desired pressure set-point, independent of the patient-hose parameters,

unintended leakages, and unknown breathing efforts. Using this control approach requires no additional calibration of the hose-filter system, which saves valuable time in the ICU of a hospital.

Furthermore, using a simulation study, it is shown that the adaptive controller achieves exact tracking and therewith improves tracking performance significantly over state-of-practice controllers. Through an experimental case study, it is shown that the controller is practically applicable. In these experiments, the adaptive controller shows an improvement in pressure tracking performance, i.e., improved rise time, less overshoot and undershoot, and faster settling times, compared to the state-of-practice linear feedback controller. Furthermore, it prevents overshoot in patient flow, which might prevent false triggers and improve patient comfort.

To improve the performance in practice, the adaptive controller could be extended to contain a quadratic hose resistance term. Furthermore, the delays in the system should be incorporated in the controller design. This might prevent the oscillations of the hose resistance estimate, resulting in improved tracking performance in practice.

In future work, other control methods should be considered to improve the control performance of mechanical ventilation further. A key example is a data-driven control method, namely, repetitive control. Repetitive control makes use of tracking errors during previously executed tasks to improve the performance in the current task. Therefore, it is particularly suitable for a repetitive process, such as ventilation.

APPENDIX
AUXILIARY LEMMAS

The lemmas presented in this section are used to prove Lemma 1 and Theorem 1 in Section IV-C. Lemmas 2–4 serve as auxiliary results to Lemma 5, in which the boundedness of $Q_{\text{out}}(t)$ is shown. First, Lemma 2 shows that $P(t)$ is always nonnegative.

Lemma 2: Consider the covariance dynamics in (26) and suppose that Assumption 1 holds. Then, $P(t) > 0$ for all $t \geq 0$.

Proof: Using (26), it can be concluded that sufficiently small positive P results in $\dot{P} > 0$. Hence, $P(t) > 0$ for all $t \geq 0$ if Assumption 1 ($P(0) > 0$) holds. □

In Lemma 3, it is proven that $|e_{\text{LS}}(t)|$ is nonincreasing (and bounded), and hence, the sign of $e_{\text{LS}}(t)$ will never change.

Lemma 3: Consider the least squares error dynamics in (27) and suppose that Assumption 1 holds. Then, $|e_{\text{LS}}(t)|$ is nonincreasing (and bounded) for all $t \geq 0$ and the sign of $e_{\text{LS}}(t)$ will never change.

Proof: The differential equation governing the dynamics of e_{LS} is given in (27), and this can be written as $\dot{e}_{\text{LS}} = -\alpha(t)e_{\text{LS}}$, with $\alpha(t) := P(Q_{\text{out}}^2(t)/m^2)$. From Lemma 2, the fact that $Q_{\text{out}}^2(t) \geq 0$, and $m^2 > 0$, and it is ensured that $\alpha(t) \geq 0$ and that $|e_{\text{LS}}(t)|$ is nonincreasing (and bounded) for all $t \geq 0$ and the sign of $e_{\text{LS}}(t)$ will never change. □

In Lemma 4, the boundedness of p_{lung} is shown.

Lemma 4: Consider the lung dynamics in (16) and suppose that Assumptions 1–3 hold. Then, $p_{\text{lung}}(t)$ is bounded for all $t \geq 0$.

Proof: First, it should be noted that p_{target} is bounded by design (Assumption 2) and $\dot{p}_{\text{pat}}$ is bounded (Assumption 3). Therefore, p_{lung} (see (16)) is bounded if, first, $(-R_{\text{leak}} - e_{\text{LS}})/(C_{\text{lung}}(e_{\text{LS}}(R_{\text{leak}} + R_{\text{lung}}) + R_{\text{leak}}R_{\text{lung}}))$ remains negative and bounded for all $t \geq 0$, note that e_{LS} is bounded (see Lemma 3) and, second, $e_{\text{LS}}(R_{\text{leak}} + R_{\text{lung}}) + R_{\text{leak}}R_{\text{lung}}$ is bounded away from zero, i.e., $|e_{\text{LS}}(R_{\text{leak}} + R_{\text{lung}}) + R_{\text{leak}}R_{\text{lung}}| > \epsilon$, for some $\epsilon > 0$, for all $t \geq 0$. If these conditions hold, $\dot{p}_{\text{lung}}$ in (16) has the opposite sign of $p_{\text{lung}}(t)$ for large enough values of $|p_{\text{lung}}(t)|$, and therefore, $p_{\text{lung}}(t)$ is bounded. The following inequalities ensure the required properties.

(I) $e_{\text{LS}}(t) > -R_{\text{leak}}\ \forall t \geq 0$.

(II) $e_{\text{LS}}(t) \geq -(R_{\text{leak}}R_{\text{lung}})/(R_{\text{leak}} + R_{\text{lung}}) + \epsilon \quad \forall t \geq 0$ for some $\epsilon > 0$.

Using Lemma 3, it is obtained that both inequalities, (I) and (II), hold for all $t \geq 0$ if these hold at $t = 0$ since the sign of e_{LS} will not change and $|e_{\text{LS}}|$ is nonincreasing. Using $e_{\text{LS}} := R_{\text{lin}} - \hat{R}_{\text{lin}}$, it is obtained that both inequalities, (I) and (II), are ensured by Assumption 1, and hence, p_{lung} is bounded for all $t \geq 0$. □

Finally, in Lemma 5, the boundedness of $Q_{\text{out}}(t)$ is ensured.

Lemma 5: Consider the output flow $Q_{\text{out}}(t)$ induced by the dynamics (17) and (18) and suppose that Assumptions 1–3 hold. Then, for all $t \geq 0$, $Q_{\text{out}}(t)$ is bounded, and hence, $Q_{\text{out}}(t) \in \mathscr{L}_\infty$.

Proof: $Q_{\text{out}}(t)$ is characterized by (17) and (18). Since p_{lung} is bounded (Lemma 4) and p_{target} is bounded by design (Assumption 2), $Q_{\text{out}}(t)$ is bounded if $e_{\text{LS}}(R_{\text{leak}} + R_{\text{lung}}) + R_{\text{leak}}R_{\text{lung}}$ is bounded away from zero for all $t \geq 0$, see the expression $Q_{\text{out}}(t)$ in (17) and (18). The latter is ensured as well, as shown in the proof of Lemma 4. Since $Q_{\text{out}}(t)$ is bounded, we also know that $Q_{\text{out}}(t) \in \mathscr{L}_\infty$. □

REFERENCES

[1] M. A. Warner and B. Patel, "Mechanical ventilation," in *Benumof and Hagberg's Airway Management*. Amsterdam, The Netherlands: Elsevier, 2013, pp. 981–997.

[2] D. M. Needham, S. E. Bronskill, J. R. Calinawan, W. J. Sibbald, P. J. Pronovost, and A. Laupacis, "Projected incidence of mechanical ventilation in Ontario to 2026: Preparing for the aging baby boomers," *Crit. Care Med.*, vol. 33, no. 3, pp. 574–579, Mar. 2005.

[3] B. Lachmann, "Open up the lung and keep the lung open," *Intensive Care Med.*, vol. 18, no. 6, pp. 319–321, Jun. 1992.

[4] M. B. P. Amato *et al.*, "Effect of a protective-ventilation strategy on mortality in the acute respiratory distress syndrome," *New England J. Med.*, vol. 338, no. 6, pp. 347–354, Feb. 1998.

[5] M. B. Amato *et al.*, "Driving pressure and survival in the acute respiratory distress syndrome," *New England J. Med.*, vol. 372, no. 8, pp. 747–755, Feb. 2015.

[6] N. Van De Wouw, B. Hunnekens, and S. Kamps, "Switching control of medical ventilation systems," in *Proc. Annu. Amer. Control Conf. (ACC)*, Milwaukee, WI, USA, Jun. 2018, pp. 532–538.

[7] B. Hunnekens, S. Kamps, and N. Van De Wouw, "Variable-Gain Control for Respiratory Systems," *IEEE Trans. Control Syst. Technol.*, vol. 28, no. 1, pp. 163–171, Jan. 2020.

[8] L. Blanch *et al.*, "Asynchronies during mechanical ventilation are associated with mortality," *Intensive Care Med.*, vol. 41, no. 4, pp. 633–641, Apr. 2015.

[9] M. Borrello, "Modeling and control of systems for critical care ventilation," in *Proc. Amer. Control Conf.*, Portland, OR, USA, Aug. 2005, pp. 2166–2180.

[10] M. Borrello, "Adaptive inverse model control of pressure based ventilation," in *Proc. Amer. Control Conf.*, Arlington, VA, USA, Jun. 2001, pp. 1286–1291.

[11] A. Pomprapa, S. Weyer, S. Leonhardt, M. Walter, and B. Misgeld, "Periodic funnel-based control for peak inspiratory pressure," in *Proc. 54th IEEE Conf. Decision Control (CDC)*, Osaka, Japan, Dec. 2015, pp. 5617–5622.
[12] M. Scheel, T. Schauer, A. Berndt, and O. Simanski, "Model-based control approach for a CPAP-device considering patient's breathing effort," *IFAC-PapersOnLine*, vol. 50, no. 1, pp. 9948–9953, Jul. 2017.
[13] H. Li and W. M. Haddad, "Model predictive control for a multi-compartment respiratory system," in *Proc. Amer. Control Conf. (ACC)*, Montréal, Canada, Jun. 2012, pp. 5574–5579.
[14] M. Scheel, A. Berndt, and O. Simanski, "Iterative learning control: An example for mechanical ventilated patients," *IFAC-PapersOnLine*, vol. 48, no. 20, pp. 523–527, 2015.
[15] D. C. Angus, M. A. Kelley, R. J. Schmitz, A. White, and J. Popovich, "Current and projected workforce requirements for care of the critically ill and patients with pulmonary disease," *JAMA*, vol. 284, no. 21, pp. 2762–2770, 2000.
[16] J. H. T. Bates, *Lung Mechanics*. Cambridge, U.K.: Cambridge Univ. Press, 2009.
[17] P. A. Ioannou and J. Sun, *Robust Adaptive Control*. Upper Saddle River, NJ, USA: Prentice-Hall, 1996.
[18] C. Olivieri, R. Costa, G. Conti, and P. Navalesi, "Bench studies evaluating devices for non-invasive ventilation: Critical analysis and future perspectives," *Intensive Care Med.*, vol. 38, no. 1, pp. 160–167, Jan. 2012.
[19] E. Fresnel, J.-F. Muir, and C. Letellier, "Realistic human muscle pressure for driving a mechanical lung," *EPJ Nonlinear Biomed. Phys.*, vol. 2, no. 1, Aug. 2014.
[20] DEMCON Macawi Respiratory Systems. (Accessed: May 3, 2019). *OEM Solutions*. [Online]. Available: https://www.macawi.com/products-services/

Joey Reinders was born in 1994. He received the B.Sc. and M.Sc. degrees in mechanical engineering from the Eindhoven University of Technology, Eindhoven, The Netherlands, in 2015 and 2017, respectively, where he is currently pursuing the Ph.D. degree with DEMCON Macawi Respiratory Systems, Enschede, The Netherlands, and the Dynamics and Control Group, Department of Mechanical Engineering, Eindhoven University of Technology, with a focus on control, learning, and automation in mechanical ventilation.

Bram Hunnekens was born in May 22, 1987. He received the B.Sc. and M.Sc. *(cum laude)* and Ph.D. degrees in mechanical engineering from the Eindhoven University of Technology, Eindhoven, The Netherlands, in 2008, 2011, and 2015, respectively. His thesis was on "performance optimization of hybrid controllers for linear motion systems."

He is currently a System Engineer with Demcon, Enschede, The Netherlands. His main research interests are on nonlinear control, performance, high-tech systems, and mechanical ventilation.

Dr. Hunnekens was a recipient of the DISC "Best Thesis Award" in 2016.

Frank Heck was born in 1994. He received the B.Sc. and M.Sc. degrees in mechanical engineering from the Eindhoven University of Technology, Eindhoven, The Netherlands, in 2015 and 2018, respectively. His M.Sc. thesis was defended at DEMCON Macawi Respiratory Systems, Enschede, The Netherlands.

Since 2018, he has been a Mechatronic System Engineer with DEMCON Macawi Respiratory Systems, where he is involved in the development of respiratory systems.

Tom Oomen (Senior Member, IEEE) received the M.Sc. *(cum laude)* and Ph.D. degrees from the Eindhoven University of Technology, Eindhoven, The Netherlands.

He held visiting positions at the KTH Royal Institute of Technology, Stockholm, Sweden, and The University of Newcastle, Callaghan, NSW, Australia. He is currently an Associate Professor with the Department of Mechanical Engineering, Eindhoven University of Technology. His research interests are in the field of data-driven modeling, learning, and control, with applications in precision mechatronics.

Dr. Oomen is also a member of the Eindhoven Young Academy of Engineering. He was a recipient of the Corus Young Talent Graduation Award, the 2015 IEEE TRANSACTIONS ON CONTROL SYSTEMS TECHNOLOGY Outstanding Paper Award, the 2017 IFAC Mechatronics Best Paper Award, and the Veni and Vidi Personal Grant. He is also an Associate Editor of the IEEE CONTROL SYSTEMS LETTERS (L-CSS), *Mechatronics* (IFAC), and the IEEE TRANSACTIONS ON CONTROL SYSTEMS TECHNOLOGY.

Nathan van de Wouw (Senior Member, IEEE) was born in 1970. He received the M.Sc. degree (Hons.) and the Ph.D. degree in mechanical engineering from the Eindhoven University of Technology, Eindhoven, the Netherlands, in 1994 and 1999, respectively.

Since 2000, he has been with Philips Applied Technologies, Eindhoven. Since 2001, he has been with the Netherlands Organisation for Applied Scientific Research (TNO), Delft, The Netherlands. He was a Visiting Professor with the University of California at Santa Barbara, Santa Barbara, CA, USA, from 2006 to 2007, the University of Melbourne, Parkville, VIC, Australia, from 2009 to 2010, and the University of Minnesota, Minneapolis, MN, USA, from 2012 to 2013. He has held a (part-time) full professor position the Delft University of Technology, Delft, from 2015 to 2019. He is currently a Full Professor with the Mechanical Engineering Department, Eindhoven University of Technology. He is also an Adjunct Full Professor with the University of Minnesota. He has published a large number of journal articles and conference papers and the books: *Uniform Output Regulation of Nonlinear Systems: A convergent Dynamics Approach* (with A. V. Pavlov and H. Nijmeijer; Birkhauser, 2005) and *Stability and Convergence of Mechanical Systems With Unilateral Constraints* (with R. I. Leine; Springer-Verlag, 2008). His current research interests are the modeling, model reduction, analysis and control of nonlinear/hybrid and delay systems, with applications to vehicular platooning, high-tech systems, resource exploration, smart energy systems, and networked control systems.

Dr. Wouw received the IEEE Control Systems Technology Award in 2015 for the development and application of variable-gain control techniques for high-performance motion systems. He is also an Associate Editor of *Automatica* and the IEEE TRANSACTIONS ON CONTROL SYSTEMS TECHNOLOGY.